Single vs multi parameter calibration for the numerical simulation of submerged flows in jet grouting applications

Stefania Evangelista, Gaspare Giovinco, and Lidia Wanik

***Abstract*—**The numerical simulation of the diffusion of turbulent submerged flows contributes to understand the fundamental mechanisms of the jet grouting technology for a more efficient use of it. In fact, the erosive efficiency of the jet, and, consequently, the dimensions of columns strongly depend on the jet propagation modalities and the energy exchange between injected and surrounding fluids. Even though the mathematical basis of turbulence models are well established, their use requires dimensionless constants to be calibrated.

In a previous study a numerical model was presented to simulate the turbulent diffusion of submerged jets. It was calibrated with literature experimental data, varying a single parameter and assuming the other ones as constant. In this work a multi-parameter calibration was carried out varying all the parameters.

The numerical results obtained with both calibrations were compared with the experimental data to evaluate the best solution in terms of accuracy and computational efficiency.

***Keywords*—** Jet grouting, Optimization, Calibration, Turbulence, Submerged flows, Numerical simulation.

I. Introduction

Ultra-high speed liquid jets are extensively used in many industrial and mining processes to cut or clean rock and rocklike materials (e.g. [1], [2]). In geotechnical engineering, this mechanism is at the base of one of the most popular ground improvement techniques, the jet grouting, currently applied worldwide in a variety of ways (e.g. [3]–[7]).

Firstly proposed in the mid sixties by a group of Japanese specialists [8], the technique is aimed at creating bodies of cemented soil via the high speed injection of water-cement mixes sometimes assisted by other fluids (air, water). The jet has the function of eroding, mixing in place and binding the soil with cement. The fluids are injected through small-diameter nozzles placed on a pipe which is continuously rotated at a constant rate and then slowly raised towards the ground surface. In this way, the jet propagates radially from the borehole axis and, after some time, the injected mortar solidifies underground, finally producing a cemented soil body of quasi-cylindrical shape (jet column) ([9], [10]). The different existing jet grouting methods are classified, according to the number of fluids injected into the subsoil, in three main categories: single (water-cement grout), double (air + grout) and triple (water + air + grout) fluid. In the double-fluid system, the grout jet is wrapped by a coaxial air jet, whereas in the triple-fluid system the grout jet is anticipated by a jet of water surrounded by air [11]. Technical improvements are continuously sought at the aim of increasing the dimensions and the mechanical properties of the jet columns (e.g. [12]).

However, due to the lack of reliable methods, the prediction of the diameter of the jet columns is still affected by a relevant degree of uncertainty and the design of jets is usually based on empirical rules [13].

For this reason the theoretical and numerical modeling of the jet grouting evolution can be useful to better understand the process (e.g. [9]–[11]).

The analysis has been here restricted to the single-fluid system, considering the complexity of the mechanical phenomena involved, but the effects of enveloping the injected fluid with a coaxial jet of air are also reproduced to investigate the principles of double and triple fluid jet grouting systems.

The first step of the analysis is devoted to the jet propagation across the space included between the nozzles and the intact soil.

The cutting fluid is ejected with high velocity from the nozzle. At the impact, the fluid threads deviate from their trajectory and tend to drag soil particles away from their original positions, with slightly different mechanisms dependent on the soil particle size [14]. Erosion takes place, therefore, with a speed depending on the combination between jet power and soil resistance ([11], [15]).

The influence radius of the jet, i.e the maximum distance at which soil can be eroded, is dictated by the capacity of the fluid threads to maintain high velocities as far as possible outside the nozzle. This feature has been investigated in the past from experimental and theoretical perspectives. Different mathematical formulations have been proposed in the literature ([16]–[18]), which, however, do not converge to a unique

Stefania Evangelista is with the Department of Civil and Mechanical Enigneering, University of Cassino and Southern Lazio, 03043 Cassino (FR), Italy (phone: +39 0776 299 4337; fax: +39 0776 299 3939; e-mail: s.evangelista@unicas.it).

Gaspare Giovinco is with the Department of Civil and Mechanical Enigneering, University of Cassino and Southern Lazio, 03043 Cassino (FR), Italy (e-mail: giovinco@unicas.it).

Lidia Wanik is with the Department of Geotechnics and Road, Silesian University of Technology, Gliwice, Poland (e-mail: Lidia.Wanik@polsl.pl).

distribution of velocity. It is, therefore, necessary to validate experimentally the predictive capability of each solution. On the other side, the available laboratory tests (e.g. [19], [20]) lead to results significantly depending on the assigned input conditions. Experimental determination of the entire distribution of the velocity field is very difficult, being the fluid ejected from small nozzles with very high speeds. As a consequence, the few available experimental studies are inadequate to completely describe the phenomenon, and provide, for instance, the distribution of velocity only along the longitudinal axis (e.g. [12]), but not in the transverse direction.

In the attempt to complete this framework, clarifying the role of the involved variables and describing with simple formulas the evolution of submerged jets, a strategy combining experiments, numerical modeling and theory has been implemented in a previous work by some of the Authors [21]. The model, calibrated with a set of experimental results has been used to perform parametric analysis varying the different input variables within the typical range of jet grouting. Simple analytical expressions from the literature have been adjusted to describe the velocity distributions along the longitudinal profile and in the cross sections at variable distances from the nozzle.

However, the model includes parameters that cannot be measured directly due to measurement limits and scale issues. As for most physically-based models which are increasingly sophisticated, calibration of parameters is a problem of great complexity, especially for large number of model parameters. Nevertheless, the success of the application of any numerical model is strongly dependent on how precisely the model is calibrated. Practitioners often count on knowledge and experience with the model to adjust the parameters through a manual trial-and-error procedure. Yet, this approach to calibration is subjective and cumbersome. Although modern hardware and software systems nowadays allow for high speed and capacity calculation, the choice of an optimal method to effectively identify the set of parameter sets is still of some concern. Automatic calibration methods, at the same time objective and easy to implement with high speed computers, have become popular in recent years.

Global optimization algorithms can efficiently search the set of parameters able to minimize (or maximize) objective functions quantifying the agreement between observations and simulations. In this work, the Authors adopted the derivative free Nelder-Mead algorithm [22] to optimize the multi-parameter calibration. This choice stems from the fact that the function to be minimized is not known in its explicit mathematical form and the iterative jacobian numerical evaluation is very expensive from a computational viewpoint, being based on fluid-dynamic numerical simulations. An "optimal" set of model parameters have been found, thus achieving the minimum defined error of the numerical results with respect to the observed experimental data.

II. Submerged Flows

Starting from the nozzle, the jet moves at very high speed (typically some hundreds meters per second) across the outer space generally filled by fluid of different origin and composition (natural groundwater, perforation water, previously injected grout, floating soil grains, etc.). At the beginning of the treatment, this fluid region is relatively thin, because the soil boundary almost coincides with the borehole surface. When the soil erosion takes place, the soil boundary shifts and the fluid region becomes larger. The evolution of the geometrical and kinematical characteristics of the jet within this zone were analyzed in the past [11] on the basis of the theory of submerged flow [16].

As the jet moves in the surrounding phase, assumed to be quiescent, part of the injected grout maintains its original direction (radial flow), either by seeping through the soil pores or by displacing the soil grains, whereas the remaining part may flow towards the ground surface (vertical flow), passing through the annular space bounded by the perforation hole and the injection stem. The measured percentage of vertical outflow, including grout and some eroded soil, increases with decreasing size of the soil grains, ranging between 0% and 80% [23].

For very pervious soils, such as coarse gravel, the vertical flow is irrelevant and almost all the injected grout is retained by the soil. In fact, the injected fluid can easily seep through the soil pores, following a nearly radial path, without significantly displacing the soil grains ([13], [24]). For finer soils, such as sands and clays, having much smaller intergranular pores, the resistance to grout seepage increases considerably. Therefore, the jet threads tend to turn back and drag the grains. In this way a complex and largely unknown erosion process takes place. In particular, two different erosion mechanisms may be postulated, for sands and clays respectively [11]. For sands, the injected fluid is assumed to penetrate by seepage into the soil pores, thus producing a significant increase of pore pressures and a corresponding reduction of the grain-to-grain contact forces, with consequent dragging action of the fluid and displacement of the soil particles ([27], [28]). For clayey soils, whose interstitial pores are very small, the jet cannot penetrate by seepage into the soil and its action is thus considered as a load imposed on the soil wall, proportional to the momentum of the jet (e.g. [15]).

In any case, the velocity profile of the jet is deeply altered along the path from the nozzle, owing to an intensive energy transfer between the injected fluid and the surrounding still soil-fluid mix. Immediately out of the nozzle all the jet threads can be approximately assumed as having constant speed and oriented along the longitudinal x-direction.

However, as the distance from the nozzle increases the speed near the jet contour decreases. This decay is due to the viscous nature of the fluid tangential stresses developing at the jet contour, which causes part of the jet energy to be transferred to the surrounding fluid. Within a small distance (starting zone) from the nozzle the velocity decay only affects

the external part of the jet cross section, but after a given distance the velocity of all the threads decreases, as shown in Fig. 1. As the jet expands the kinetic energy dissipates as diffusion [29]. The nozzle diameters are very small (typically from 2 to 6 mm), and thus the extension of the starting zone is very limited (in the order of few centimeters) and not influent on the erosive capacity of the jet. The analysis of jet propagation becomes, on the contrary, relevant in the diffusion zone where much of the soil erosion takes place.

The turbulence also causes that part of the surrounding fluid is entrained into the jet, with a consequent increase of the flow rate. The velocity in each point of the turbulent field can be seen as sum of a mean component, obtained by integrating the velocity vector in a sufficiently long time interval, and a fluctuation component randomly variable with time. While the fluctuation velocity has uncertain direction and intensity, the mean one is stationary, it is the predominant one and has a paramount importance on the cutting ability of jet.

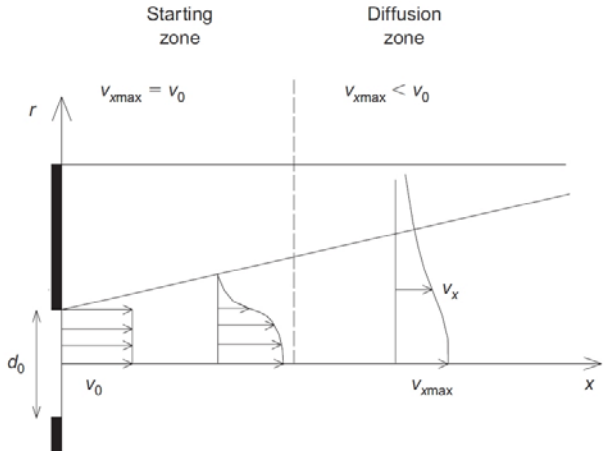

Fig. 1 velocity distribution and pattern of submerged jet [9]

[12] experimentally observed that the attenuation of the fluid velocity along the jet axis is affected by the nozzle size and shape (see also [30]). In particular, a very sharp reduction of maximum longitudinal velocity is produced by a sudden narrowing of the nozzle cross-sectional area, whereas a lower rate of velocity decrease occurs when the entry and exit section of the nozzle are gently connected by a cone.

The velocity pattern in each cross-section is characterized by a bell-shaped surface, providing positive values of the mean velocity along x even for infinite distances r from the jet axis. However, it seems more realistic to assume that the jet is confined inside a conical region, and that the velocity falls to zero at the border of such cone. For the sake of simplicity, however, it is assumed that, for a given value of x, the velocity of the jet threads is constant in the whole cross-section and equal to a mean equivalent value.

Concerning viscosity, cement-water suspensions are usually treated in terms of equivalent Newtonian fluids, by defining an apparent viscosity independent of the fluid velocity, although it is known that they behave more like Bingham fluids [31]. Furthermore, because of the cement hydration, a variation of the apparent viscosity should be expected with time, but this can be neglected if the period between the preparation and the injection of the grout is relatively short [11].

III. Numerical Model and Calibration Procedure

In the attempt to investigate the evolution of submerged jets, a strategy combining experiments, numerical modeling and theory has been implemented.

Numerical simulations of submerged jets have been performed with a finite-volume model in Fluent (Ansys Fluent, vers. 6.1, 2003) managed by a further code in Scilab [32]. The computational domain (600-mm high and 1200-mm long) has been discretized into a finite number of cells with quadrangular basis, as shown in Fig. 2, on which the general equations of conservation (transport) are integrated.

The domain, which includes the nozzle and the surrounding volume, is symmetric along the jet axis and much wider than the diffusion zone of the jet, in order to limit the boundary effects on the analysis results. The jet mainly flows in the horizontal direction, so the upper wall has been considered impervious, as well as the boundary above the nozzle, whereas the front wall has been assumed permeable, with a constant hydraulic head (Fig. 2).

The calculation area delimited by these borders has been subdivided by a squared mesh (Fig. 2) of variable dimension: smaller clusters (0.6 mm side size) have been created near the nozzle to better catch the variability of velocities, whereas larger dimensions (with a maximum width of 2 mm) have been progressively assigned while moving away from the nozzle. The final mesh has been selected after a large number of trial-and-error tests, aimed at optimizing the computational effort in relation with the accuracy and stability of the obtained solution.

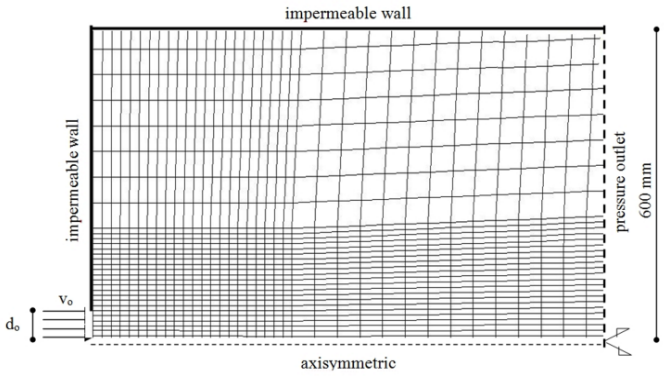

Fig. 2 sketch of the computational domain with the adopted mesh and the boundary conditions (not to scale)

In order to simplify the model, the fluid injected from the nozzle has been assumed to have the same composition and physical characteristics of the fluid filling the surrounding space. Although the inertial effects and buoyancy of the two fluids are different in reality, the fluid in which the jet occurs typically consists of underground water, floating soil particles

and previously injected fluid(s). The differences between the rheological characteristics of the two fluids are not significant and the assumption is, therefore, acceptable.

Although in the literature several different turbulence models are also available (e.g. [33], [34]) the classical *k-ε* model has been selected and applied in this work, being it the most widely adopted for this kind of problems.

The fluid behavior has been described through the *k-ε* turbulence model, that in steady-state conditions can be written as (1) [35]:

$$\rho(\mathbf{u}\cdot\nabla)\mathbf{u} = \nabla\cdot\left[-p\cdot\mathrm{I}+(\mu+\mu_T)\left(\nabla\mathbf{u}+(\nabla\mathbf{u})^T\right)+ -\frac{2}{3}(\mu+\mu_T)(\nabla\cdot\mathbf{u})\mathbf{I}-\frac{2}{3}\rho k\mathbf{I}\right]+\mathbf{F}$$

$$\nabla\cdot\mathbf{u}=0$$

$$\rho(\mathbf{u}\cdot\nabla)k = \nabla\cdot\left[\left(\mu+\frac{\mu_T}{\sigma_k}\right)\cdot\nabla k\right]+P_k-\rho\varepsilon \qquad (1)$$

$$\rho(\mathbf{u}\cdot\nabla)\varepsilon = \nabla\cdot\left[\left(\mu+\frac{\mu_T}{\sigma_\varepsilon}\right)\cdot\nabla\varepsilon\right]+C_{\varepsilon_1}\frac{\varepsilon}{k}P_k-C_{\varepsilon_2}\rho\frac{\varepsilon^2}{k}$$

$$\mu_T=\rho C_\mu\frac{k^2}{\varepsilon}$$

$$P_k=\mu_T\left[\nabla\mathbf{u}:\left(\nabla\mathbf{u}+(\nabla\mathbf{u})^T\right)-\frac{2}{3}(\nabla\cdot\mathbf{u})^2\right]-\frac{2}{3}\rho k\nabla\cdot\mathbf{u}$$

where ρ is the fluid density, μ is the laminar dynamic viscosity, μ_T is the turbulent viscosity, p is the fluid pressure, $\mathbf{u}$ is the fluid velocity vector, k is the turbulent kinetic energy, ε is the turbulent kinetic energy dissipation rate.

The coefficients $\sigma_k, \sigma_\varepsilon, C_\mu, C_{\varepsilon_1}, C_{\varepsilon_2}$ are to be tuned by a comparison with experimental data [19].

The *κ-ε* model has been particularized in the range of velocities typical of jet grouting, calibrating its parameters with the above shown data of [19].

The simple algorithm (e.g. [36]) has been applied to solve equations and compute the velocity fields. A detailed description of the numerical model can be found in the Fluent manual [37]. More details on the numerical scheme can be found in [21].

In the previous work by [21], however, after a preliminary sensitivity analysis, the following values (suggested by the authors) have been fixed for the coefficients $\sigma_k, \sigma_\varepsilon, C_\mu, C_{\varepsilon_2}$:

$\sigma_k = 1.0$, $\sigma_\varepsilon = 1.3$, $C_\mu = 0.145$ and $C_{\varepsilon 2} = 1.92$,

whereas the parameter C_{ε_1}, which governs the kinetic energy dissipation rate ε, was changed until the longitudinal profiles observed in the experiments were captured. Different values of C_{ε_1} were necessary to fit experimental results with numerical curves for different initial velocities. Specifically, an exponential dependence of C_{ε_1} with the Reynolds' number Re was found [21], with values of C_{ε_1} in the range of interest close to 1.655, substantially agreeing with the literature values for similar applications (e.g. [38]).

In this work, instead, a better calibration for the whole set of parameters $\sigma_k, \sigma_\varepsilon, C_\mu, C_{\varepsilon_1}, C_{\varepsilon_2}$ has been sought.

Moreover, since the complete geometry of the nozzle is unknown, the definition of the turbulence condition at the water inlet is also affected by uncertainty. Two more parameters, referring to the turbulent kinetic energy and dissipation rate at the nozzle ($\sigma_{k_0}, \sigma_{\varepsilon_0}$), have been added, therefore, to take into account this feature and to evaluate the corresponding turbulence condition. In the single-parameter calibration, instead, both parameters have been fixed equal to 1.

In order to find the optimal values of the whole set of coefficients, the authors solved the following minimization problem in Scilab [32] through the Nelder-Mead algorithm (2) [22]:

$$min\left(\sum_{i=1}^{N}\left(v_{num,i}\left(C_\mu, C_{\varepsilon 1}, C_{\varepsilon 2}, \sigma_k, \sigma_\varepsilon, \sigma_{k_0}, \sigma_{\varepsilon_0}\right)-v_{exp,i}\right)^2\right) \qquad (2)$$

where the index *i* refers to the specific considered measured value and v_{exp} and v_{num} are the experimental and numerical axial velocity values, respectively, obtained from the data of [19] and from the finite-volume code.

Since the number of experimental points is small compared with the number of the optimization parameters, the authors added to the measured values two more equally-spaced velocity values obtained from a cubic interpolation of the measured ones (Fig. 3), for each interval between two consecutive measured values. The optimal number of the interpolated values was determined by the authors from a sensitivity analysis on the multi-parameter calibration and verifying the stability of the single-parameter calibration once this new values were added. Unfortunately, the lack of uncertainty values corresponding to the measured velocities from [19] did not allowed the authors to operate a regression instead of an interpolation using a more accurate functional relationship.

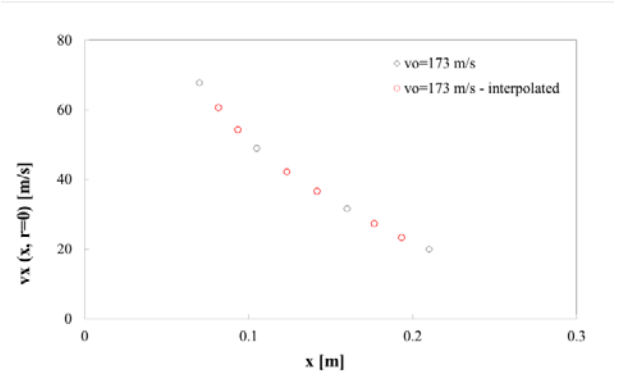

Fig. 3 experimental and interpolated reference values used for the model calibration for an initial value of velocity of 173 m/s

The optimal set of parameters was obtained by coupling the Scilab solver with simulations in Fluent [39].

The parameter values were changed in the journal file and then the Fluent solver calculated the corresponding solution (the axial velocities) until the minimum root mean square value between experimental and numerical axial velocities was reached.

The flowchart of the optimization procedure is reported in Fig. 4.

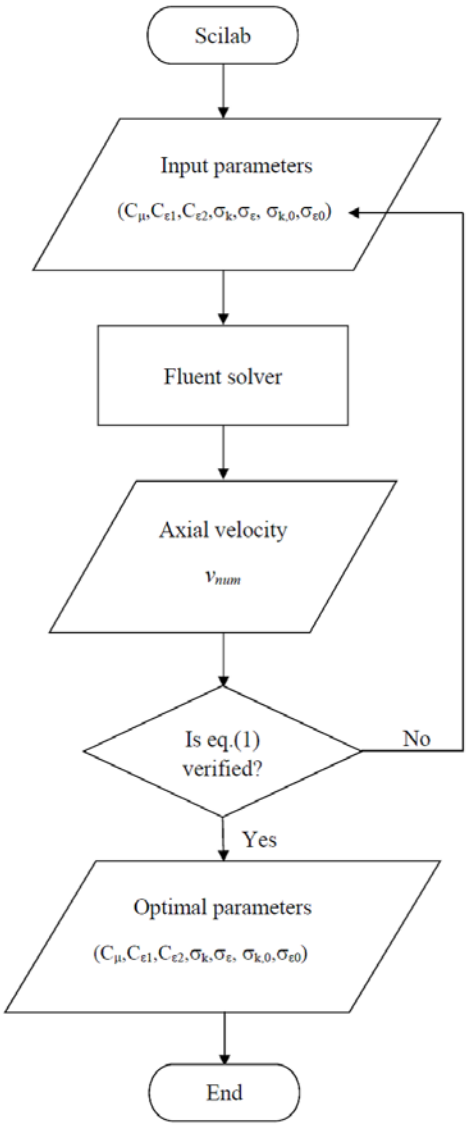

Fig. 4 flowchart describing the whole optimization procedure

IV. Results

The numerical results obtained through multi-parameter calibration, compared against single-parameter calibration and experimental data by [19], are plotted in Fig. 5 for the following values of velocity at the nozzle exit: 173.2, 200.0, 223.61, 244.95, 264.58, 282.84 m/s, respectively. Dashed and continuous lines represent single-parameter and multi-parameter calibration, respectively.

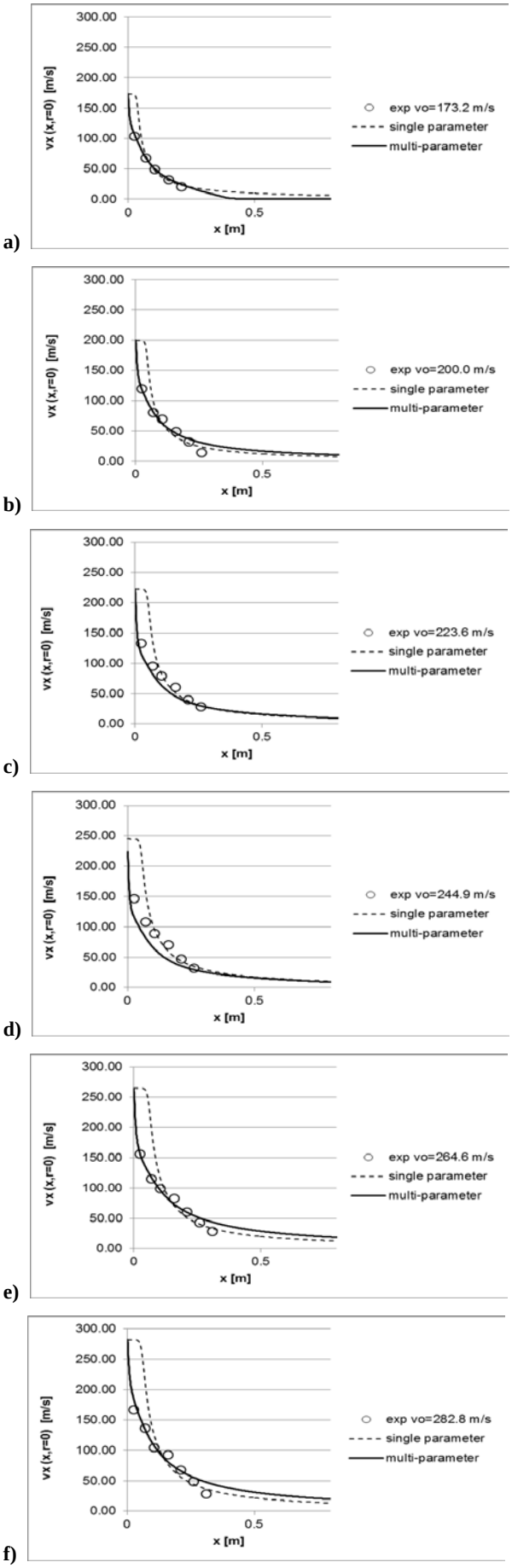

Fig. 5 comparison of the numerical results, calculated with both single-parameter (dashed line) and multi-parameter (continuous line) calibration, with the experimental data [19] for the following values of velocities, respectively: a) 173.2, b) 200.0 c) 223.6, d) 244.9, e) 264.6, f) 282.8

The numerical results obtained through the multi-parameter calibration (continuous line) in comparison with the experimental data [19] are then summarized for the entire set of velocities in Fig. 6.

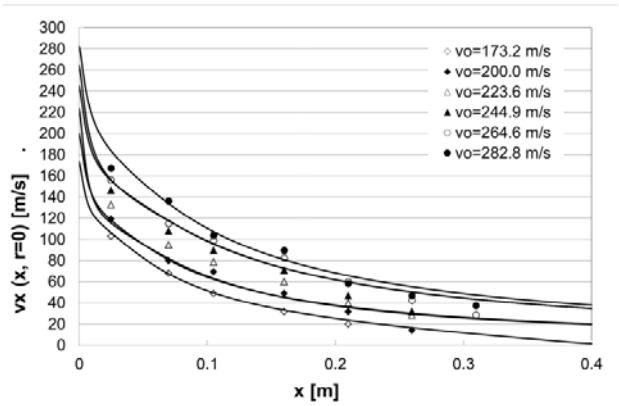

Fig. 6 summary of the comparisons of the numerical results calculated with the multi-parameter calibration (continuous line) against the experimental data [19] for the entire set of velocities

The values of the main parameters obtained through the numerical multi-parameter calibration are reported in Table 1 for the different values of velocities.

Table 1: Model parameters value obtained through multi-parameter calibration

v_o [m/s]	*173.2*	*200.0*	*223.6*	*244.9*	*264.6*	*282.8*
C_μ	0.128	0.0153	0.0184	0.00882	0.00766	0.0107
C_{ε_1}	0.000387	0.465	0.000382	0.553	0.585	0.729
C_{ε_2}	1.90	0.842	1.24	0.787	0.809	0.534
σ_k	0.169	2.74	11.1	3.94	3.60	1.91
σ_ε	0.00367	0.0694	0.0225	0.0727	0.0896	0.0916

In Fig. 7, instead, the values of each calibrated parameter of the model obtained through the numerical multi-parameter calibration are plotted as functions of the considered different values of velocity.

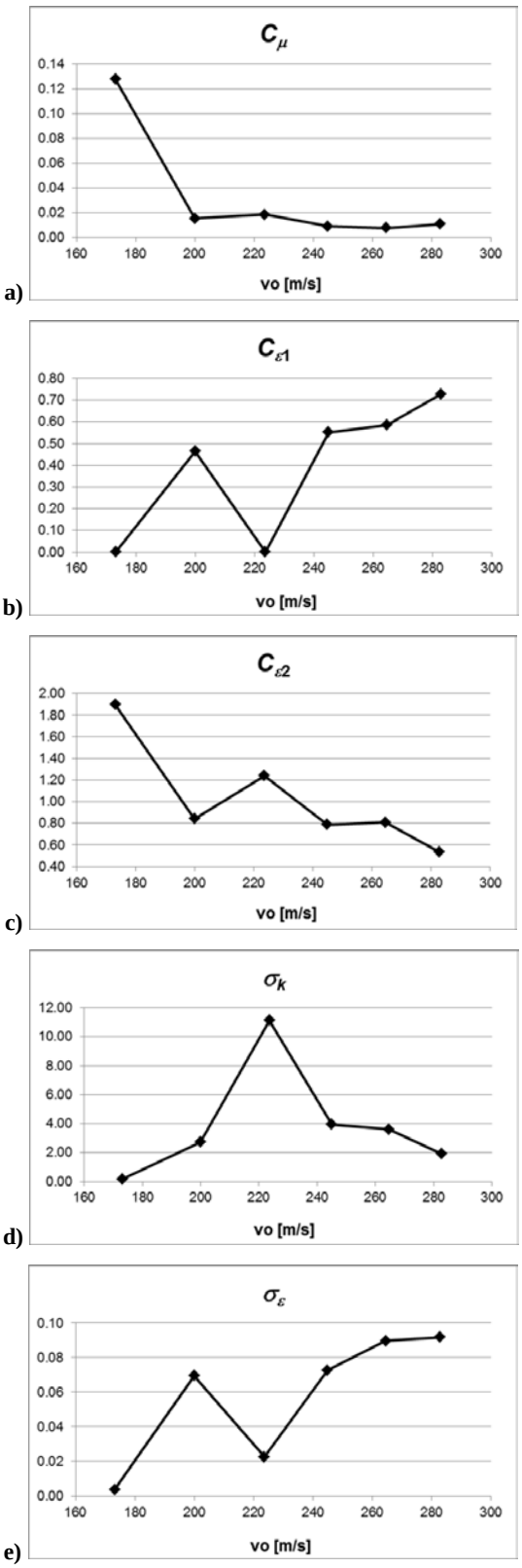

Fig. 7 values of the model parameters obtained through the multi-parameter calibration for the different velocity values

By defining the absolute percentage error *e* as (3):

$$e\% = \frac{V_{num} - V_{\exp}}{V_{\exp}} \cdot 100 \quad (3)$$

it is possible to obtain the plots in Fig. 8.

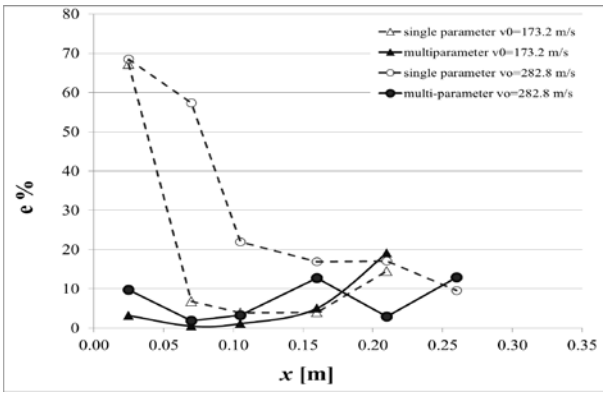

Fig. 8 comparison of the absolute percentage errors obtained through single and multi-parameter calibration respectively

As shown by Figs. 5 and 6, both single and multi-parameter calibration provide a good agreement with the experimental data of [19]. The multi-parameter optimization allows a better simulation of the experimental results near the nozzle. It also gives absolute percentage errors smaller than the ones obtained by the single-parameter calibration for small values of the longitudinal abscissa *x*, whereas at larger distances from the nozzle single- and multi-parameter calibrations give similar values of the errors (Fig. 8).

Depending on the specific aim of the numerical analysis, therefore, the optimization technique has to be selected taking into account that a higher accuracy can be achieved through the multi-parameter calibration, although the single-parameter calibration is computationally simpler and more efficient.

V. Conclusion

In the present paper the authors compared the results of single and multi-parameter calibration of the closure constants of the k-ε turbulence model used in a numerical finite volume model simulating the turbulent diffusion of submerged jets.

The multi-parameter optimization shows better results in comparison with the experimental ones near the nozzle, whereas at larger distances from the nozzle single- and multi-parameter calibrations give similar values of the errors.

The optimization technique, therefore, has to be selected in turn on the basis of the specific aim of the numerical analysis, taking into account that the multi-parameter calibration offers a higher accuracy, whereas the single-parameter calibration is computationally simpler and more efficient.

Acknowledgment

The Authors intend to thank Prof. Giuseppe Modoni for the precious suggestions and discussions on the topic.

References

[1] W. Farmer, and P.B. Attewell, "Rock penetration by high velocity jet", in *Proc. Int. Journal of Rock Mechanics & Mining Sciences*, vol. 2, pp. 135-153, 1965.

[2] D.A. Summers, *Waterjetting technology*, E & FN Spon, London, UK, 1995.

[3] M. Iwasaki, "Application of water jet for drilling rock undersea", Turbomachinery, vol. 17, no. 12, pp. 761-767, 1989 [in Japanese].

[4] P. Croce, and G. Modoni, "Design of jet grouting cutoffs", *Ground Improvement*, vol. 10, no. 1, pp. 1-9, 2005.

[5] G.P. Lignola, A. Flora, and G. Manfredi, "A simple method for the design of jet-grouted umbrellas in tunneling", ASCE *J Geotech Geoenviron*, vol. 134, no. 12, pp.1778-1790, 2008.

[6] G. Modoni, and J. Bzówka, "Analysis of foundations reinforced with jet grouting", ASCE *J Geotech Geoenviron*, vol. 138, no. 12, pp. 1442-1454, 2012.

[7] N. Eramo, G. Modoni, M. Arroyo Alvarez de Toledo, "Design control and monitoring of a jet grouted excavation bottom plug", in Proc. *7th Int. Symposium on Geotechnical Aspects of Underground Construction in Soft Ground*, TC28 IS Rome, Viggiani ed., Taylor & Francis Group London, 16-18 May 2011, pp. 611-618, 2012.

[8] T. Yahiro, and H. Yoshida, "Induction grouting method utilizing high speed water jet", in *Proc. VIII Int. Conf on Soil Mechanics and Foundation Engineering*, Moscow (Russia), pp. 402-404, 1973.

[9] A. Flora, G. Modoni, S. Lirer, and P. Croce, "The diameter of single-, double- and triple-fluid jet grouting columns: Prediction method and field trial results", *Géotechnique*, vol. 63, no. 11, pp. 934-945, 2013.

[10] M. Ochmanski, G. Modoni, and J. Bzówka, "Prediction of the diameter of jet grouting columns with artificial neural networks", *Soil & Foundations*, 2014.

[11] G. Modoni, P. Croce, and L. Mongiovì, "Theoretical modelling of jet grouting", *Géotechnique*, vol. 56, no. 5, pp. 335-347, 2006.

[12] M. Shibazaki, "State of practice of jet grouting", in *Proc. 3rd Int. Conf. on Grouting and Ground Treatment*, ASCE Geotech. Special Pubbl. vol. 120, no. 1, pp. 198-217, 2003.

[13] P. Croce, and A. Flora, "Analysis of single fluid jet-grouting", *Géotechnique*, vol. 50, no. 6, pp. 739-748, 2000.

[14] P. Croce, A. Flora, and G. Modoni, *Jet grouting: technology, design and control*, Taylor & Francis Group, CRC press, London, 2014.

[15] A.A: Dabbagh, A.S. Gonzalez, and A.S. Pena, "Soil erosion by a continuous water jet", *Soils and Foundations*, vol. 42, no.5, pp.1-13, 2002.

[16] J.O. Hinze, *Turbulence*, 2nd ed., New York, McGraw-Hill, 1975.

[17] G.N. Abramovich, *The theory of turbulent jets*, MIT Press, Cambridge, Massachusetts, US, 1963.

[18] P.A. Davidson, *Turbulence*, Oxford, UK, Oxford University Press, 678 p, 2004.

[19] H. de Vleeshauwer, and G. Maertens, "Jet-grouting: State of the art in Belgium", in *Proc. Conference Grouting - Soil improvement - Geosystem including reinforcement*, Finnish Geotechnical Society, Helsinki, pp.145-156, 2000.

[20] M. Di Natale, and R. Greco, "Misure di velocità in un getto sommerso ad asse verticale mediante la tecnica PIV", in *Proc. Symposium promoted by Associazione Italiana di Anemometria Laser* (AIVELA), Ancona, Ottobre 2000, 2000 [in Italian].

[21] G. Modoni, L. Wanik, G. Giovinco, J. Bzowka, and A. Leopardi, "Numerical analysis of submerged flows for jet grouting", *Ground improvement*, vol. 4, pp. 1-12, 2015.

[22] J.A. Nelder, and R. Mead, "A Simplex Method for Function Minimization", *The Computer Journal*, 1965.

[23] J.L. Kauschinger, R. Hankour, and E.B. Perry, "Methods to estimate composition of jet-grout bodies", in *Grouting, Soil Improvement, and Geosynthetics*, ASCE Geotechnical Special Publication (GSP), vol. 30, pp. 169-181, 1992.

[24] G. Miki, and W. Nakanishi, "Technical progress of the jet grouting method and its newest type", in *Proc. Int. Conf. on in Situ Soil and Rock Reinforcement*, Paris, Oct. 9-11, pp. 195-200, 1984.
[25] M. Shibazaki, *State-of-the-art grouting in Japan: Grouting and Deep Mixing*, vol. 2, pp. 851-867, 1996.
[26] C.S. Covil, and A.E. Skinner, "Jet grouting: A review of some of the operating parameters that form the basis of the jet grouting process", *Grouting in the Ground*, London, United Kingdom, Thomas Telford, pp. 605-627, 1994.
[27] B. Bergschneider, and B. Walz, "Jet grouting – range of the grouting jet" in *Proc. XIII European Conf. on Soil Mech. and Found. Engineering*, Vanicek et al. eds Prague, pp. 53-56, 2003.
[28] J. Stein, and J. Graβe, "Jet grouting tests and simulation", in *Proc. 13th Eur. Conf. Soil Mech. Geotech. Eng*, Prague, pp. 899-902, 2003.
[29] W.-H. Lam, G. Hamill, D. Robinson, R. Raghunathan, and C. Kee, "Submerged Propeller Jet", in Proc. of *WSEAS/IASME Int. Conf. on Fluid Mechanics* (FLUIDS '05), Udine, Italy, January 20-22, 2005, ISBN: 960-8457-08-4.
[30] D.V. Cavaropol, "The advance experimental and numerical studies of water turbulent jets", in *Proc. of WSEAS Int. Conf. on Development, Energy, Environment, Economics* (DEEE '10), Puerto De La Cruz, Tenerife, November 30-December 2, 2010, ISBN: 978-960-474-253-0.
[31] H.F. Winterkorn, and H. Fang, *Foundation Engineering Handbook*, Van Nostrand, New York, 1975.
[32] Scilab Enterprises, Scilab: Free and Open Source software for numerical computation, 2012. Version 5.5.2. http://www.scilab.org.
[33] D. Wilcox, *Turbulence modelling for CFD*, DCW Industries, Inc., 2000.
[34] L. Kalmár, "Numerical investigation of fully-developed turbulent flows in two-dimensional channel by stochastic turbulent model", in *Proc. 3rd WSEAS International Conference on Engineering Mechanics, Structures, Engineering Geology* (EMESEG '10), Corfu Island, Greece, July 22-25, 331-336, 2010.
[35] B.E. Launder, and D.B. Spalding, "The numerical computation of turbulent flows", *Computer, Methods in Applied Mechanics and Engineering*, vol. 3, pp. 269-289, 1974.
[36] S.V. Patankar, *Numerical heat transfer and fluid flow*, Taylor and Francis, London, UK, 1980.
[37] Fluent, Fluent 6.1 User's Guide. Fluent Inc., 2003.
[38] E.J. Smith, G.J. Nathan, and B.B. Dally, "Range of validity of a modified K-Epsilon model of the non reacting flow from a precessing jet nozzle", in *Proc. 3rd Int. Conf. on CFD in the Minerals and Process Industries* - CSIRO, Melbourne, Australia, December 10-12, pp. 499-504, 2003.
[39] S. Evangelista, G. Giovinco, G. Modoni, and L. Wanik, "Optimization for multi-parameter calibration in the numerical analysis of submerged flows for jet grouting", in *Proc. 8th WSEAS International Conference on Environmental and Geological Science and Engineering* (EG '15), Italy, June 27-29, 2015.

Stefania Evangelista was born in Cassino (FR), Italy, in 1978. She got her M.Sc. degree (with honors) in Civil Engineering in 2006 at University of Cassino and Southern Lazio, where she started right after her PhD, finished in 2010. She collaborated with "University "Federico II" of Napoli, Italy, and the "National Center for Computational Hydroscience and Engineering" (NCCHE), University of Mississippi, Oxford, MS, where she spent almost two years, as Visiting Scholar first and then as Research Assistant.

She is currently a Research Assistant at University of Cassino and Southern Lazio, Department of Civil and Mechanical Engineering. Her main research topics (both numerical and experimental) are in the fields of River Hydraulics (modeling of free-surface flows, sediment transport and bed evolution, also in unsteady conditions, e.g. dam breaks) and Water Networks (water hammer, water quality and infrastructure protection against contamination risk). She is the main author and co-author of several papers published in national and international conference proceedings and journals.

Dr. Evangelista is member of International Association for Hydro-Environment Engineering and Research (**IAHR**) and Italian Hydraulic Group (**GII**).